COMPOSITIONAL CHARACTERISTICS OF THE ARISTARCHUS CRATER FROM (M^3) DATA. J. F. Mustard[1], C. M. Pieters[1], P. J. Isaacson[1], J. W. Head[1], R. L. Klima[1,3], N. E. Petro[4], M. Staid[5], J. M. Sunshine[6], C. Runyon[7], L. A. Taylor[8]. [1]Brown University Geological Sciences, Box 1846, Providence, RI 02912, [2]USGS Denver, [3]APL, [4]NASA Goddard, [5]PSI, [6]Univ. of MD, [7]College of Charleston, [8]Univ of Tenn. [John_Mustard@Brown.edu].

Introduction: The crater Aristarchus and the plateau that it straddles have long been targets of inquiry, due to their unique combination of brightness, geologic complexity, abundance of linear rilles, large dark mantle deposits, and with the advent of multispectral imaging data, spectral diversity [e.g. 1, 2, 3, 4]. The craters sites astride the southeastern edge of the plateau and excavates both material from the plateau and the mare deposits of Oceanus Procellarum [4]. The Moon Mineralogy Mapper (M^3) [5] provides a new opportunity to investigate the compositional characteristics of this important near-side crater. Here we show the first results of the nature of the compositional diversity for Aristarchus crater.

Data and Methods: M^3 is an imaging spectrometer covering the 0.43-3.0 μm wavelength region in 260 spectral bands and a spatial resolution of up to 70 m/pixel. M^3 flew on the Chandrayaan-1 spacecraft and operated until August 2009. M^3 acquired data in several modes including full spectral and spatial resolution but acquired near global data in a reduced resolution mode of 85 spectral bands and 140 m/pixel. The M^3 data are calibrated to radiance using prelaunch and inflight coefficients and divided by the solar spectrum and the cosine of the incidence angle to apparent reflectance [6]. Refinement of the calibration is ongoing. Here we analyze two global-mode M^3 strips that cover the Aristarchus crater (M3G20090 209T054030 and M3G20090209T072710) (Figure 1).

To facilitate rapid analysis of the diversity of the spectral properties of the surface, we calculate spectral parameters that summarize key absorption features. Three of these are shown in Figure 2 for the Aristarchus crater: 1 μm integrated band depth (sum of band depths between 0.79 and 1.3 μm), 2 μm integrated band depth (sum of band depths between 1.66 and 2.5 μm) and the ratio between the UV and the visible (0.42/0.75 μm).

From the regions exhibiting the maximum in spectral diversity as shown by the parameter map in Figure 2, we select representative reflectance spectra. Spectra are selected from homogeneous areas and averages of on the order 3 lines and 3 samples are collected. Residual calibration artifacts are present in the data and these can be minimized by ratioing the spectra of a region of spectrally unremarkable material, such as typical lunar highlands soil. Because of the push broom design of M3, artifacts are commonly particular to columns in the detector. Thus in selecting highland soils for the purposes of ratioing, spectra are selected from areas in the same columns.

Results: The Aristarchus crater is well covered by the two M3 strips as shown in Fig. 1. The spectral diversity as shown in Figs. 2 and 3 is quite remarkable. In the color ratio composite (Fig. 2), areas rich in olivine appear green while areas rich in pyroxene appear yellow-pink. The blue-magenta regions have a stronger UV-VIS ratio. Regions with weak to absent absorptions represented by these ratios appear dark.

Reflectance spectra from regions showing the most mineral diversity are shown in Fig. 3. These spectra show the distinct mafic mineral absorption bands characteristic of olivine and pyroxene, with both low- and high-Ca pyroxene distinguished. The Aristarchus Plateau is a well-known Dark Mantle Deposit (DMD), and M^3 spectra of DMD show absorptions characteristic of glass.

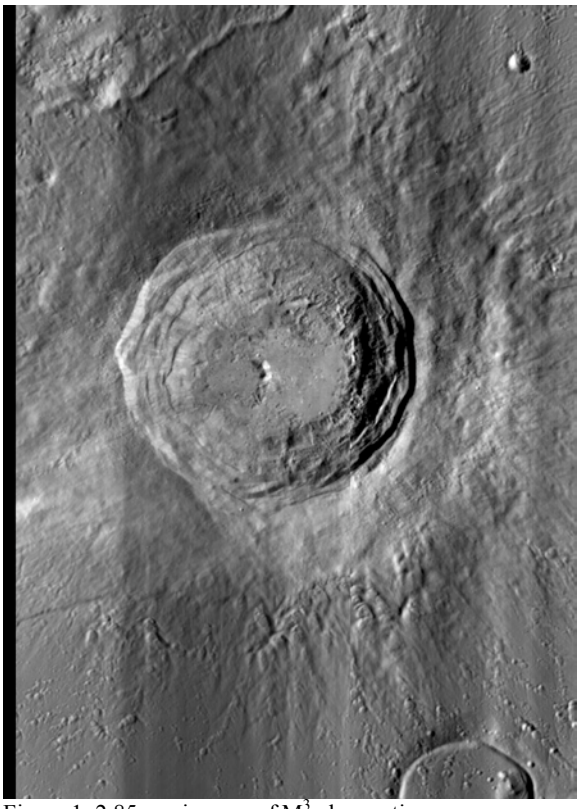

Figure 1. 2.85 μm images of M^3 observations M3G20090209T054030 and M3G20090209T072710

There is a clear distinction between the northern half and southern half of the crater. The southern half is clearly enriched in olivine, while the northern half shows a greater presence of pyroxene. The central peaks show weak absorptions, largely restricted to a weak 1 µm band, and a strong UV-VIS slope. The southern half of the crater also shows large patches in the ejecta that are devoid of mafic mineral signatures (appears dark in Figure 2).

The distribution of olivine confirms what was shown by telescopic [3] and Clementine data [7] with a large deposit exterior to the crater on the southeast rim and small patches distributed on the walls and in the ejecta. The distribution of olivine interior to the crater is characterized by linear bands that run up the crater wall and continue to the exterior beyond the crater rim, but not apparently beyond the extent of the continuous ejecta, perhaps analogs to rays. This same distribution is observed in regions enriched in pyroxene on the

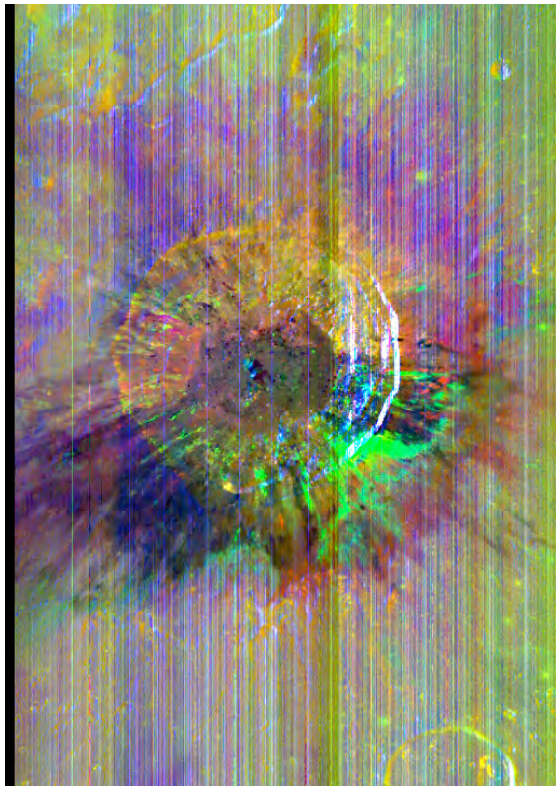

Figure 2. Color ratio composite showing integrated 2 µm band depth in red, integrated 1 µm band depth in green and UV-VIS ratio in blue.

northern half of the crater, but less distinctly.

The mafic signatures in the northern half of the crater are typical of low-Ca pyroxene while those exterior to the crater in the mare basalts are typical of high-Ca pyroxene or olivine-bearing basalts.

Conclusions: This first look at the M^3 data for this region show a large diversity of mineralogic signatures

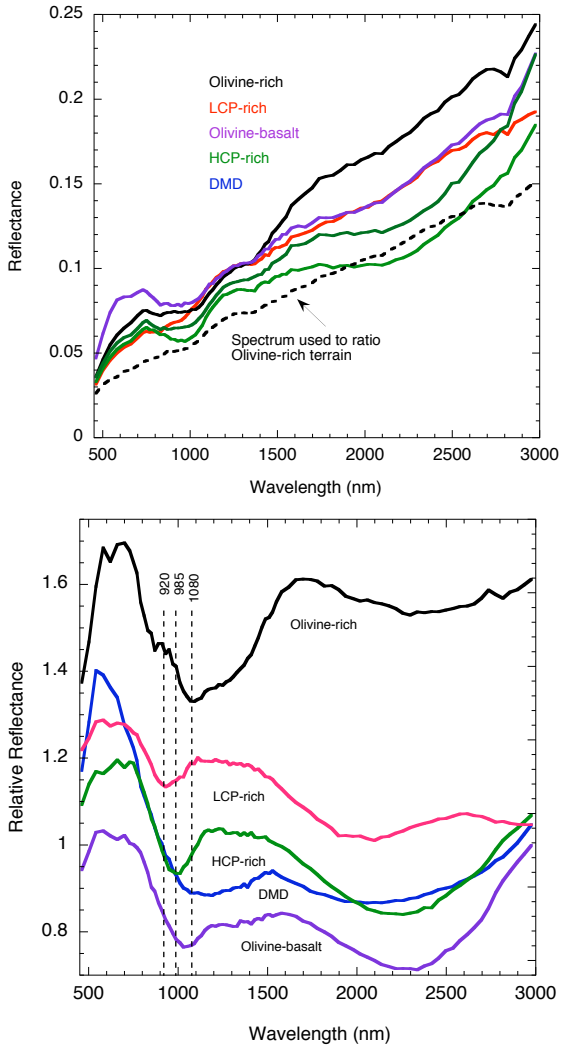

Figure 3. (top) M^3 reflectance spectra showing a diversity of materials. LCP refers to low-Ca pyroxen, HCP refers to high-Ca pyroxene, DMD refers to dark mantle deposit. (bottom) The same spectra as in the top panel ratioed to mature highland soils as described in the text to better display the mineral absorption features. Example of typical mature highland soil used to ratio is show in the top graph

representative of diverse rock types as noted by others [e.g. 3, 4, 7]. We will be refining the mineralogic and lithologic interpretations, including analysis of olivine Mg# [8].

References: [1] Guest, J.E. (1973) Geol. Soc. Am. Bull. **84**, 2873-2894 [2] Head, J.W. (1974) PLPSC Geochem. Cosmochim Acta 1 (suppl.) 207-222. [3] Hawke et al. (1995) Proc. Lunar Sci. Conf. **26**, 559-560. [4] Chevrel et al. (2009) Icarus **199**, 9-24. [5] Pieters et al. (2009) **3226**, 568-572 [6] Green et al. (2009) LPSC, **40**, abstract 2307 [7] LeMouelic et al. (1999) GRL **26**, 1195-1198. [8] Isaacson, P. et al., (2010) LPSC **41** (this conference).